Clinical Neurophysiology xxx (xxxx) xxx

Contents lists available at ScienceDirect

Clinical Neurophysiology

journal homepage: www.elsevier.com/locate/clinph

Cortico-cortical evoked potentials of language tracts in minimally invasive glioma surgery guided by Penfield stimulation

Kathleen Seidel [a,1,*], Jonathan Wermelinger [a,1], Pablo Alvarez-Abut [a,1], Vedran Deletis [b,c], Andreas Raabe [a], David Zhang [a], Philippe Schucht [a]

[a] Department of Neurosurgery, Inselspital, Bern University Hospital, University of Bern, Bern, Switzerland
[b] Department of Neurosurgery, University Hospital Dubrava, Zagreb, Croatia
[c] Albert Einstein College of Medicine, New York, NY, USA

HIGHLIGHTS

- Cortico-cortical evoked potentials (CCEPs) were obtained in minimally invasive resection for glioma in awake and asleep patients.
- Optimal stimulation and recording sites were guided by awake Penfield stimulation and analyzed in real time during surgery.
- CCEP features were affected by tumor location and histopathology, and correlated with postoperative aphasia.

ARTICLE INFO

Article history:
Accepted 23 December 2023
Available online

Keywords:
Arcuate fascicle
Brain mapping
Cortico-cortical evoked potentials
Glioma
Intraoperative neurophysiological monitoring

ABSTRACT

Objective: We investigated the feasibility of recording cortico-cortical evoked potentials (CCEPs) in patients with low- and high-grade glioma. We compared CCEPs during awake and asleep surgery, as well as those stimulated from the functional Broca area and recorded from the functional Wernicke area (BtW), and vice versa (WtB). We also analyzed CCEP properties according to tumor location, histopathology, and aphasia.

Methods: We included 20 patients who underwent minimally invasive surgery in an asleep-awake-asleep setting. Strip electrode placement was guided by classical Penfield stimulation of positive language sites and fiber tracking of the arcuate fascicle. CCEPs were elicited with alternating monophasic single pulses of 1.1 Hz frequency and recorded as averaged signals. Intraoperatively, there was no post-processing of the signal.

Results: Ninety-seven CCEPs from 19 patients were analyzed. There was no significant difference in CCEP properties when comparing awake versus asleep, nor BtW versus WtB. CCEP amplitude and latency were affected by tumor location and histopathology. CCEP features after tumor resection correlated with short- and long-term postoperative aphasia.

Conclusion: CCEP recordings are feasible during minimally invasive surgery. CCEPs might be surrogate markers for altered connectivity of the language tracts.

Significance: This study may guide the incorporation of CCEPs into intraoperative neurophysiological monitoring.

Abbreviations: A, Astrocytoma IDH mutated; AC, Anterior commissure; A.C., Alternating current; ACP, Anterior Commissure Point; AF, Arcuate fascicle; AUC, Area under the curve; Av, Averages; Bp, Bipolar; BtW, Broca to Wernicke; CCEP, Cortico-cortical evoked potential; DTI, Diffusion tensor imaging; FL, Frontal lobe; fMRI, Functional magnetic resonance imaging; FT, Fiber tracking; GB, Glioblastoma IDH wild type; HGG, High-grade glioma; IDH, Isocitratdehydrogenase; IFOF, Inferior fronto-occipital fascicle; IL, Insular lobe; LGG, Low-grade glioma; M, Metastasis; MNI, Montreal Neurological Institute; MRI, Magnetic resonance imaging; N/r, Not reported; nTMS, Navigated transcranial magnetic stimulation; O, Others; OG, Oligodendroglioma IDH mutated, 1p/19q codeleted; On/off, Online/offline analysis; PC, Posterior commissure; PL, Parietal lobe; PW, Pulse width; SD, Standard deviation; SLF, Superior longitudinal fascicle; SSEP, Somatosensory evoked potential; TL, Temporal lobe; WHO, World health organization; WtB, Wernicke to Broca.

* Corresponding authors at: Department of Neurosurgery, Inselspital Bern University Hospital, University of Bern, Bern, Switzerland.
E-mail address: kathleen.Seidel@insel.ch (K. Seidel).

[1] These authors contributed equally and share the first authorship.

https://doi.org/10.1016/j.clinph.2023.12.136
1388-2457/

1. Introduction

The oncological challenge during neurosurgical tumor resection is to achieve maximal resection while preserving the functional integrity of the patient's language system (Hamer et al., 2012). Preservation of essential language pathways remains a crucial and difficult task. Intraoperative neuropsychological and neurophysiological testing of the patients during awake surgery has become part of clinical routine in many experienced centers following the pioneering work of experts (Berger and Ojemann, 1992; Duffau et al., 2003a; Spena et al., 2017; Szelényi et al., 2010). However, awake speech mapping during an open-skull procedure is stressful for the patient, and patient compliance typically decreases over the course of the tumor resection (Nossek et al., 2013). Patients with high-grade glioma and peritumoral edema might be even more challenging (Nossek et al., 2013). Thus, a neurophysiological marker of the integrity of the arcuate fascicle (AF) and other language tracts to enable continued monitoring in such situations would be a valuable adjunct. Several groups have sought additional techniques to avoid having to abandon the surgical procedure in such circumstances. Advanced imaging techniques combined with preoperative navigated transcranial magnetic stimulation have become useful tools to guide surgery (Krieg et al., 2017; Stieglitz et al., 2012). However, those methods provide information either about anatomical data or preoperatively acquired functional mapping data and do not allow for real-time monitoring of function during surgery.

In the neurosurgical context, Matsumoto et al. were the first to demonstrate the feasibility of recording evoked potentials from temporal language sites when stimulating frontal language hubs and vice versa. They called these signals cortico-cortical evoked potentials (CCEPs) (Matsumoto et al., 2004). The CCEP comprises several components, including peaks called N1 and N2 (Vincent et al., 2017). While initially only performed in awake epilepsy patients with implanted subdural grids (Matsumoto et al., 2017), some groups have been studying the applicability of this technique to glioma surgery in awake (Saito et al., 2014; Saito et al., 2022; Suzuki et al., 2019; Tamura et al., 2016; Vega-Zelaya et al., 2023; Yamao et al., 2014; Yamao et al., 2017; Yamao et al., 2021) and even asleep patients (Giampiccolo et al., 2021a; Kang et al., 2023; Kanno et al., 2018; Nakae et al., 2020; Saito et al., 2014; Suzuki et al., 2019; Vega-Zelaya et al., 2023; Yamao et al., 2014, 2017, 2021). However, intraoperative real-time recordings of CCEPs are still a technical challenge, which often requires careful signal processing to differentiate them from artifacts.

The objective of our study was to evaluate the feasibility of intraoperative recording of real-time CCEPs in a cohort of glioma patients undergoing minimally invasive surgery in an asleep-awake-asleep setting. We guided strip electrode placement by classical Penfield stimulation of positive cortical language sites and preoperative fiber tracking of the AF. We also compared the quality of CCEPs obtained during the awake and asleep phases. Intraoperatively, there was no post-processing of the signal, and the feedback was immediately available to the surgeon. Finally, we compared CCEP properties according to tumor location, histopathology, sex, and aphasia.

2. Methods

This study was approved by the local ethics committee (BASEC 2023-00311). All patients included gave their consent for further use and publication of their anonymized data.

2.1. Patient population and surgical technique

Patients scheduled for maximal safe tumor resection of a speech-eloquent glioma were included in this study from 10/2019 to 04/2023. The patients needed to be eligible for an awake craniotomy involving either a frontal or temporal language area, and have a suspected diagnosis of either a low- or high-grade glioma. Preoperative diffusion tensor imaging (DTI) fiber tracking (Brainlab® algorithm) was performed to visualize the AF in relation to the tumor. The surgical technique was an asleep-awake-asleep setting with local scalp blocks. Further details of our anesthesia protocol and perioperative anti-epileptic drug administration are described elsewhere (Spena et al., 2017). The size of the craniotomy was chosen according to the tumor location, following a minimally invasive approach, with a craniotomy centered over the tumor. Preoperative, postoperative and follow-up language performance was clinically classified according to whether patients had aphasia or not. Intraoperative testing was performed by a trained speech therapist who had evaluated the patient before surgery. Intraoperative neurophysiological recordings were made by a trained neurophysiologist and were instantly available on a screen to the surgical team. However, the surgical strategy was not modified according to the information provided by the recorded CCEP. Histopathology was postoperatively classified according to the 2021 world health organization (WHO) classification (Louis et al., 2021). For the 2 patients operated on before 2021, we used the previous WHO classification; both had glioblastoma, isocitratdehydrogenase (IDH) wild type.

2.2. Penfield stimulation

Penfield stimulation for mapping of language function was performed with an ISIS IOM System (Inomed®, Emmendingen, Germany). We applied square-wave biphasic current with a pulse width (PW) of 600 ms and a frequency of 50 Hz, using a bipolar stimulation probe with an interpolar distance of 8 mm and tip diameters of 2 mm (Inomed® REF 522 624). The stimulation current intensity was determined over the primary motor area of the tongue while the patient was counting, to check for dysarthria. This stimulation intensity, an average of 3–6 mA, was then used for further mapping of the speech eloquent cortex. We called the frontal functional language hubs "Broca's area" (Keller et al., 2009) and the temporal and parietal functional language hubs "Wernicke's area" (Binder, 2015), respectively. During the cortical mapping, electrocorticography was recorded to detect after-discharges or spike activity with the help of subdural spider electrodes (AdTech® REF VG04A-IS00X-0KG).

2.3. Stimulation and recording of CCEPs

The CCEP recordings were performed directly after the cortical Penfield stimulation. If possible, they were carried out prior to the surgical cortical incision and continued while the patient was asleep (during resection of non-eloquent language areas or immediately after finishing tumor resection). Additionally, CCEPs were obtained in the asleep phase, but the strip location had already been determined in the initial awake phase with the support of Penfield stimulation.

CCEP stimulation and recording were performed with the same ISIS IOM System (Inomed, Emmendingen, Germany) using cortical strip electrodes of 4 contacts (AdTech ® REF MS04R-IP10X-0JH, diameter 5 mm, distance between centers 10 mm). Strip electrodes were placed on the speech areas identified by Penfield stimulation. If a speech area was outside the field of view, the DTI fiber tracking of the AF and anatomical landmarks were used to determine the approximate location and the strip electrode was pushed under the dura under neuronavigational guidance. One strip was used at the stimulation site, and 1 or 2 strips were positioned at the recording site (Fig. 1). During the initial step, the frontal lobe strip was used for stimulation of Broca's area and the temporal lobe

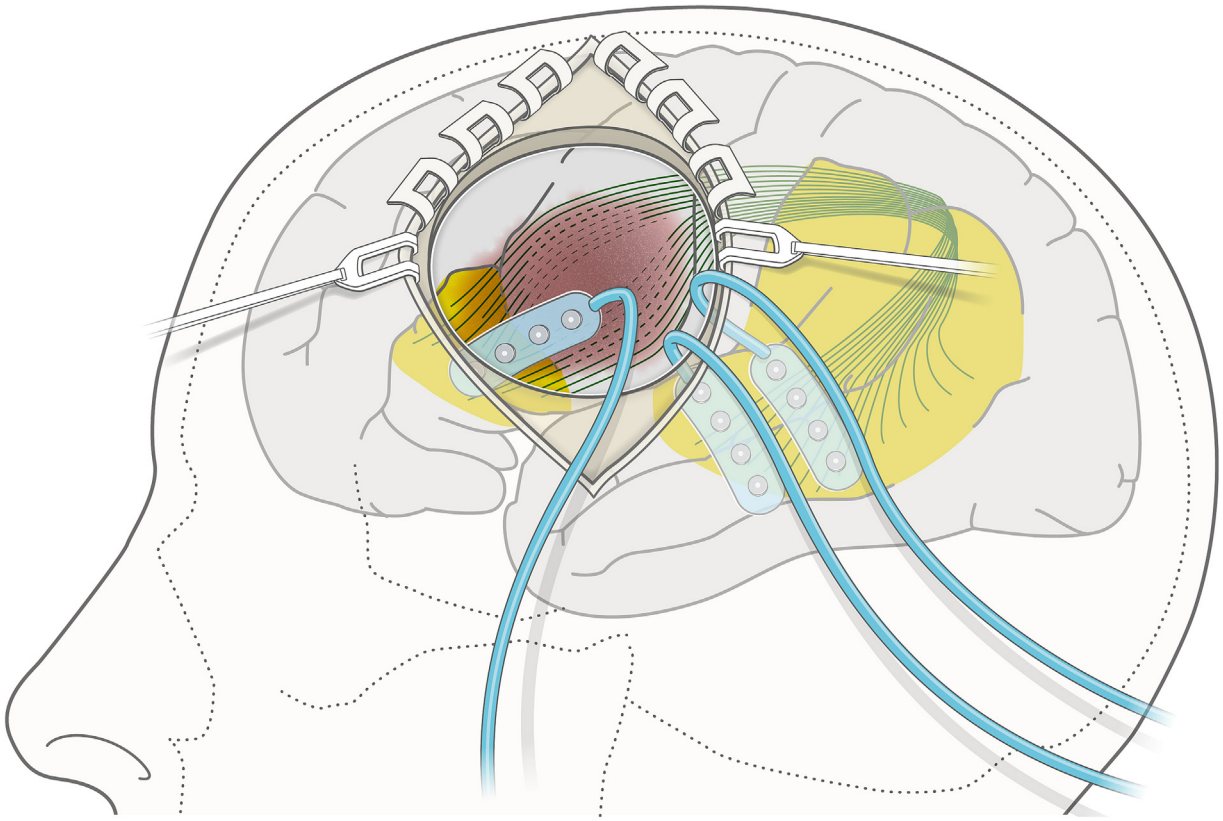

Fig. 1. Intraoperative setting for CCEP recordings. Schematic of the minimally invasive approach of a craniotomy with cortex exposure only above the tumor location. Due to the small size, the stimulation and recording strips (blue) are partially pushed under the dura to target terminations of the AF (green) or other language tracts. Eloquent speech hubs including Broca's and Wernicke's area are illustrated in yellow; the infiltrative tumor extending to the Broca area, central region and AF is indicated in brown. AF: arcuate fascicle, CCEP: cortico-cortical evoked potential. © Inselspital, Bern University Hospital, Dept. of Neurosurgery.

strips for recording on Wernicke's area, as described by Matsumoto et al. (2004). In more than half of the cases, stimulation for CCEPs was additionally performed at the temporal lobe while recording from the frontal lobe.

The stimulation was carried out with 2 adjacent contacts of the stimulating strip (bipolar stimulation). The recordings were both bipolar (with 2 adjacent contacts of the strip) and referential. For referential recordings, the contralateral mastoid was used as reference. The reason for using bipolar recordings was to compare the signal-to-noise ratio with referential recordings. The stimulation was carried out with alternating monophasic square waves of constant-current, single-pulse electrical stimulation, with a PW of 0.5 ms, a stimulation intensity of 12–30 mA, and a stimulation frequency of 0.9–1.1 Hz. The recordings were acquired with a hardware high-pass filter of 0.5 Hz in 2 patients and 30 Hz in 17 patients, a hardware low-pass filter of 5 kHz, an epoch of 200–1000 ms and a sampling rate of 20,000 Hz. On the NeuroExplorer software, the filters were set at 10 for high-pass and 1500 for low-pass, while the sensitivity was 50–300 μV/Div and the sweep 200–300 ms for online visualization. Two repeated trials of 30–60 averages each were recorded when a reproducible waveform was observed.

During the acquisition of the recordings, we performed online data analysis to evaluate the efficacy of the strip electrode placement by comparing CCEP amplitudes and reproducibility when obtained with different pairs of stimulating electrodes. If needed, recording and stimulating electrodes were repositioned to enable us to obtain the most reliable CCEP responses.

2.4. Data analysis

The data were grouped according to whether the patient was asleep or awake during the recording and either stimulated via electrodes located in Broca's area and recorded from electrodes located in Wernicke's area (Broca to Wernicke, BtW) or the other way around (Wernicke to Broca, WtB). In this way we tried to obtain bidirectional recordings of CCEPs. For each of the 4 combined settings (BtW-awake, WtB-awake, BtW-asleep, and WtB-asleep) we selected the optimal referential and bipolar recording (depending on the best available responses and repeatability) from each patient for further analysis. If possible, we included both trials of this best recording for each setting. The data from the 2 patients with a hardware high-pass filter of 0.5 Hz were excluded from the statistical analysis due to lack of comparability.

N1 was defined as a negative deflection occurring at a peak latency between approximately 10 and 30 ms and with a duration of at least 10 ms, as determined by visual inspection. If, instead, there was a notable positive deflection in this time frame, the signal (i.e., the whole trace) was inverted for analysis. Accordingly, P1 and P2 were defined as notable positive deflections preceding and following N1, respectively, whereas N2 was defined as a notable negative deflection following P2, with a peak latency of 30 to 120 ms, depending on the first complex (i.e., P1, N1, and P2). A CCEP was defined as a signal containing a clear N1 (upon visual inspection). We visually inspected all the CCEPs included for the presence or absence of P1, P2, and N2 and determined their onset and peak latencies using the NeuroExplorer software.

Custom-made Python 3 scripts were used to analyze the CCEP data offline. Latency, amplitude, and frequency content were determined.

What we call the N1 or Matsumoto amplitude corresponds to the amplitude of the N1 described by Matsumoto et al. (see (Matsumoto et al., 2004), Fig. 1). A straight line is drawn between either the onset of N1 or the peak P1 to either the end of the first complex or the peak P2, and the amplitude is defined as the difference between the peak N1 value and the value on the line at the N1 peak latency. The N1 area under the curve (AUC) was defined as the area between the CCEP trace and the line that was just described. The amplitude of the N2 was defined as the difference between the peak N2 value and the peak P2 value. The main frequency of a CCEP was defined as the frequency at which the Fourier transform of the CCEP (as a time series) has the maximum absolute value. The Fourier transform was obtained using the *fft* function from Python package *scipy.fftpack*.

Statistical analysis was performed using the Python packages *scipy.stats* and *statsmodels*. Statistical significance was set at $p < 0.05$. Student's t-tests or Mann-Whitney U tests were carried out to compare the mean values of 2 groups, depending on whether or not the data were normally distributed. Additionally, ANOVA or Kruskal-Wallis tests were used to compare mean values for more than 2 groups, and for post-hoc analysis, either the Bonferroni or the Tukey test was used, depending again on whether or not the data were normally distributed.

The recording-setting groups were awake versus asleep and BtW versus WtB. Restricting CCEPs to the awake or asleep setting, we also compared BtW with WtB, and restricting to BtW or WtB, we compared awake with asleep. For the different recording settings, the peak latencies of P1, N1, P2, and N2 were analyzed, as well as the N1 and N2 amplitude, the N1 area under the curve (AUC), and the main frequency.

For further analysis, data were grouped according to clinical parameters: sex (female, male), history of seizures (yes, no), tumor histopathology (IDH wild type glioblastoma, IDH mutated astrocytoma, 1p/19q codeleted oligodendroglioma), tumor grade (low-grade glioma i.e., WHO grade 2; high-grade glioma i.e., WHO grade 3 and 4) and tumor location (frontal, temporal, insular, temporo-insular). To study the effect of preoperative, postoperative, and follow-up aphasia (yes, no), the CCEP data were further split according to the time of recording (before, during, or after resection). For these different clinical groups, the N1 and N2 peak latencies, as well as the N1 and N2 amplitudes, were compared.

All values are presented as (mean ± standard deviation).

2.5. Visualization of cortical stimulation points

If data points had been intraoperatively acquired by neuronavigation using the Brainlab software (Brainlab AG, Germany), we retrospectively classified speech errors during Penfield stimulation into six categories: speech arrest with no further specification, naming errors, phonemic paraphasias, semantic paraphasia, speech hesitation or slowing, and non-specific errors. Navigation points were considered only for the selected CCEPs.

For further analysis, we manually identified the Anterior Commissure (AC) and Posterior Commissure (PC) using axial and sagittal T1 magnetic resonance imaging (MRI) sequences. The location of cortical stimulation points was measured based on their x, y, and z coordinates relative to the Anterior Commissure Point (ACP). An age-matched cohort was downloaded from the IXI database (https://brain-development.org/ixi-dataset/, (Kuklisova-Murgasova et al., 2011)) and normalized into the Montreal Neurological Institute (MNI) space using a linear probabilistic transformation (Ashburner and Friston, 2005). AC/PC coordinates from each stimulation point were transformed into MNI coordinates and projected onto the MNI brain for visualization. Data analysis was performed with Brainstorm (https://neuroimage.usc.edu/brainstorm, (Tadel et al., 2011)), which is documented and freely available for download online under the GNU general public license.

Only those cases in which stimulation and recording sites were available for the same CCEP during the retrospective data analysis of the navigation points were used for illustration.

3. Results

3.1. Clinical data

We attempted CCEP recordings in 20 patients and obtained reliable signals in 19 (95%). The one patient from whom no CCEPs could be obtained had a tumor that predominantly involved the parietal cortex. Intraoperative Penfield stimulation was unsuccessful in this patient due to inability to cooperate. In 11 patients, we observed speech disturbance elicited by Penfield stimulation in the exposed Broca's area, in 6 patients in the exposed Wernicke's area, and in 2 patients in both.

Table 1 shows the characteristics of the patients in which CCEPs were successfully elicited and recorded (including the 2 patients with different filters). Twenty-five percent of the patients had low-grade glioma and 75% high-grade glioma. The cohort included 9 patients with glioblastoma, IDH wild type; 8 with astrocytoma, IDH mutated (grade 2, 3 or 4), and 3 with oligodendroglioma 1p/19q codeleted, IDH mutated (grade 2 and 3). Overall, 37% of patients had a pure frontal and 37% a pure temporal tumor location, whereas 26% involved the insula. Before surgery, 47% of patients had no aphasia, 47% had mild aphasia, and only 1 patient had severe preoperative aphasia. For each patient, the detailed information of histopathology and WHO grade, tumor location, history of preoperative seizures, pre- and postoperative language deficits are specified in Supplementary table S1.

We attempted CCEP recordings during the awake phase in 17 patients and successfully recorded reliable CCEPs in 16 (94%). We tried to obtain CCEPs in the asleep phase in 13 cases and made

Table 1
Clinical data.

Mean age at surgery (years)	46 (n = 19)
Sex	Female (n = 5) Male (n = 14)
Histopathology	Oligodendroglioma IDH mutated 1p/19q codeleted (n = 3) Astrocytoma IDH mutated (n = 8) Glioblastoma IDH wild type (n = 8)
WHO grade	Low-grade, grade 2 (n = 5) High-grade, grade 3 and 4 (n = 14)
History of seizures	Yes (n = 14) No (n = 5)
Tumor location	Frontal (n = 7) Temporal (n = 7) Insula (n = 1) Temporo-insular (n = 4)
Aphasia (pre-op / post-op/ follow up)	No (n = 9/6/12) Yes (n = 10/13/7)
CCEP recordings (successful/ attempted)	Awake (n = 16/17) Asleep (n = 9/13) BtW (n = 18/20) WtB (n = 7/13) Referential (n = 15/20) Bipolar (n = 18/20)

BtW: Broca to Wernicke, CCEP: cortico-cortical evoked potential, IDH: Isocitratdehydrogenase, n: number of patients in whom CCEPs were obtained, WtB: Wernicke to Broca.

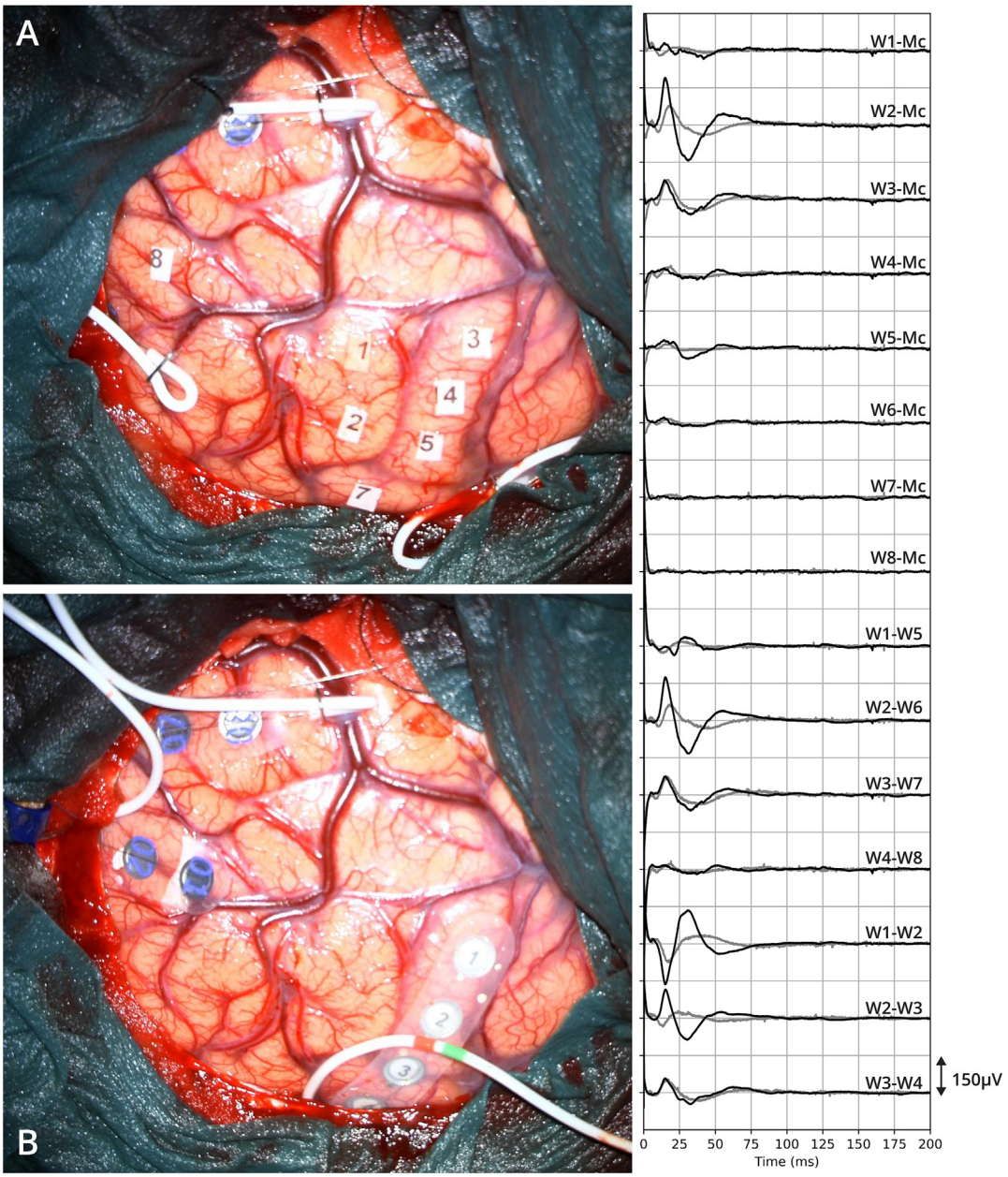

Fig. 2. Illustrative case. Left: Microscope images with paper marks indicating where speech errors were obtained after Penfield stimulation (A) and the adjusted strip position (B) of patient number 14. Right: Sample of recorded traces of the same patient during resection (black) and after resection (grey) both under general anaesthesia. Paper mark 2 indicates the functional face motor area as determined by Penfield stimulation. The illustrated CCEPs are elicited by stimulation through contact B3 and B4 of the frontal strip (bottom of the microscope image) which was positioned on the spot of paper mark 5 (speech arrest) and 7 (phonemic paraphasia). The highest signal amplitude was obtained on contact W2 of the temporal strips in the upper left corner of the microscope image, which corresponds to paper mark 8 (speech arrest). The CCEP cascade indicates the highest N1 amplitude on contact W2 against the reference (Mc: Mastoid) and further, a phase reversal between contacts W1-W2 and W2-W3. The N1 amplitude decreased and the N1 latency increased on contact W2 after resection. Directly after surgery there was a severe worsening of language performance, which finally resolved to a better performance than the pre-operative status in the follow-up consultation (see also table S1 of the supplements for the exact type of language deficits). B: Broca, CCEP: cortico-cortical evoked potential, Mc: mastoid, W: Wernicke. © Inselspital, Bern University Hospital, Dept. of Neurosurgery.

reliable recordings in 9 (69%). Concerning the direction, we stimulated BtW in all 20 patients and recorded reliable and repeatable CCEPs in 18 (90%). For WtB, we attempted CCEPs in 13 cases and were successful in 7 (54%). Not all channels recorded positive responses and some contacts had higher amplitudes than others (Fig. 2). The success rate was 75% for referential recordings and 90% for bipolar recordings.

3.2. CCEP properties

The CCEP data of 17 patients were analyzed. A total of 97 CCEPs were selected for further analysis. Depending on availability and the quality of reliable and repeatable recording in the different settings (awake vs asleep; BtW vs WtB; bipolar vs referential recordings), patients each contributed between 1 and a maximum of 12 CCEPs to the dataset (out of 16 possible CCEPs per patient). In most patients, there were more recordings that were successful; however, we chose to focus on the best signals for each setting (one channel per paradigm, two consecutive trials). The selection process yielded 58 CCEPs in the awake setting, 34 asleep, 5 while falling asleep, 70 from BtW, and 27 from WtB; 44 were referential whereas 53 were bipolar recordings. Fig. 3 shows a sample CCEP for each of the 4 recording settings (BtW-awake, WtB-awake, BtW-asleep, WtB-asleep), and Table 2 summarizes the main prop-

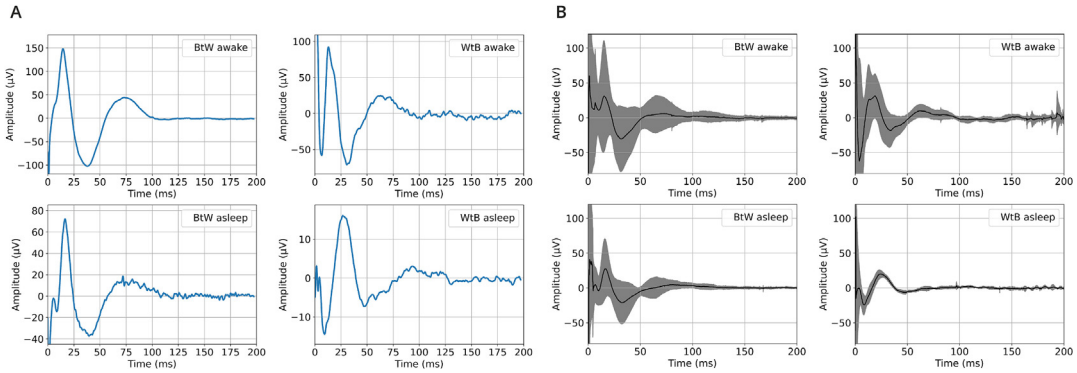

Fig. 3. CCEP traces in different settings. A) Sample CCEPs recorded in awake and asleep patients, from BtW and WtB, low-pass filtered at 500 Hz for visualization. These are typical examples of waveforms with N1 and N2 potentials. Note the different scales on the y-axis. B) Average of all CCEPs included for analysis in the different settings (black line), plus and minus the standard deviation at each time-point (gray-shaded area). The narrower envelope in the asleep compared to the awake phase might be due to either the smaller sample size in the asleep group, or to greater stability of the signal in this setting. BtW: Broca to Wernicke, CCEP: cortico-cortical evoked potential, WtB: Wernicke to Broca. © Inselspital, Bern University Hospital, Dept. of Neurosurgery.

Table 2
CCEP properties overall.

	Overall
P1 peak latency (ms)	11.78 ± 3.84 (*n* = 74) min: 4.3 max: 26.0
N1 peak latency (ms)	21.13 ± 6.7 (*n* = 97) min: 12.8 max: 44.4
P2 peak latency (ms)	36.37 ± 10.29 (*n* = 89) min: 21.6 max: 65.1
N2 peak latency (ms)	71.18 ± 17.8 (*n* = 72) min: 35.5 max: 115.0
N1 Matsumoto amplitude (μV)	64.47 ± 51.31 (*n* = 97) min: 7.6 max: 226.9
N2 amplitude (μV)	59.43 ± 44.81 (*n* = 69) min: 4.58 max: 186.77
N1 AUC (μV*ms)	779.12 ± 718.25 (*n* = 97) min: 31.48 max: 4652.32
Main frequency (Hz)	20.89 ± 8.56 (*n* = 97) min: 5.08 max: 50.79

mean ± standard deviation; AUC: area under the curve, CCEP: cortico-cortical evoked potential, n: number of CCEPs.

erties of all the CCEPs included for analysis. Of the CCEPs included, 74 had a P1, 89 a P2, and 72 an N2 potential. Patient 16 had comparably long N1 latencies (up to 44.4 ms), but since the waveforms fitted the expectations from previously observed CCEPs, we decided to include them as is. Furthermore, 30 CCEPs were recorded in females and 67 in males; 6 were recorded before, 38 during, and 53 after resection. Supplementary document S1 illustrates all included CCEP recordings. Supplementary table S2 contains all analyzed features. Supplementary figure S1 shows two illustrative MRIs and MNI brains with projected stimulation and recording sites.

3.3. CCEPS and stimulation settings

Overall, there was no significant difference either in N1 peak latency between awake (20.4 ± 6.8 ms) and asleep (22.2 ± 6.9 ms) states or between BtW (21.4 ± 7.2 ms) and WtB (20.5 ± 5.0 ms). There was also no significant difference in N1 amplitude between awake (71.4 ± 59.4 μV) and asleep states (51.1 ± 33.6 μV) or between BtW (66.3 ± 53.8 μV) and WtB (59.8 ± 44.0 μV).

In the BtW setting, there was no statistically significant difference in latency, amplitude, AUC, and frequency content between CCEPs recorded in awake or asleep states. In the WtB setting, there was a significant difference between N1 peak latency, P2 peak latency, N2 peak latency, and N2 amplitude in awake and asleep states (see Table 3). Furthermore, in the awake setting, a significant difference between BtW and WtB was found in N2 peak latency (Student's t-test, $p = 0.0004$) and main frequency (Student's t-test, $p = 0.017$). In the asleep setting, there was a significant difference between BtW and WtB in N1 peak latency (Mann-Whitney, $p = 0.03$).

3.4. CCEPS and clinical data

N1 peak latency of CCEPs from patients with IDH wild type glioblastoma (24.4 ± 8.2 ms) tended to be significantly longer than that from patients with IDH mutated astrocytoma (18.0 ± 3.5 ms), but there was no difference compared to patients with 1p/19q codeleted oligodendroglioma (20.5 ± 4.3 ms) (Kruskal-Wallis,

Table 3
CCEP properties from Broca's area to Wernicke's area and vice versa, awake versus asleep.

	Broca to Wernicke (BtW)			Wernicke to Broca (WtB)		
	Awake	Asleep	p-value	Awake	Asleep	p-value
P1 peak latency (ms)	12.8 ± 4.33 (*n* = 25)	11.37 ± 3.73 (*n* = 26)	0.12 (b)	11.15 ± 3.03 (*n* = 11)	9.32 ± 0.86 (*n* = 8)	0.14 (a)
N1 peak latency (ms)	21.32 ± 7.59 (*n* = 39)	21.22 ± 7.33 (*n* = 26)	0.70 (b)	18.4 ± 4.0 (*n* = 19)	25.31 ± 3.43 (*n* = 8)	0.0004* (a)
P2 peak latency (ms)	36.11 ± 10.93 (*n* = 39)	38.37 ± 11.7 (*n* = 24)	0.13 (b)	30.87 ± 5.93 (*n* = 15)	43.43 ± 3.72 (*n* = 6)	0.0002* (a)
N2 peak latency (ms)	73.53 ± 17.26 (*n* = 29)	78.27 ± 17.37 (*n* = 19)	0.37 (a)	55.01 ± 10.93 (*n* = 16)	89.47 ± 3.21 (*n* = 3)	0.00008* (a)
N1 Matsumoto amplitude (μV)	72.73 ± 63.82 (*n* = 39)	54.92 ± 36.98 (*n* = 26)	0.55 (b)	68.73 ± 49.1 (*n* = 19)	38.5 ± 12.61 (*n* = 8)	0.11 (a)
N2 amplitude (μV)	76.86 ± 54.99 (*n* = 29)	51.33 ± 34.41 (*n* = 17)	0.10 (a)	46.49 ± 22.76 (*n* = 15)	8.61 ± 2.86 (*n* = 3)	0.02* (a)
N1 AUC (μV*ms)	890.65 ± 954.81 (*n* = 39)	642.48 ± 465.81 (*n* = 26)	0.44 (b)	754.47 ± 580.75 (*n* = 19)	693.91 ± 292.19 (*n* = 8)	0.66 (b)
Main frequency (Hz)	20.57 ± 8.68 (*n* = 39)	18.36 ± 7.59 (*n* = 26)	0.30 (a)	26.73 ± 9.0 (*n* = 19)	20.31 ± 3.59 (*n* = 8)	0.07 (a)

mean ± standard deviation, (a) Student t-test, (b) Mann-Whitney U test, *significant at $p < 0.05$. Note that some CCEPs were recorded while the patient was falling asleep. The total number of awake and asleep CCEPs included for analysis is 92. AUC: area under the curve, BtW: Broca to Wernicke, CCEP: cortico-cortical evoked potential, n: number of CCEPs, WtB: Wernicke to Broca.

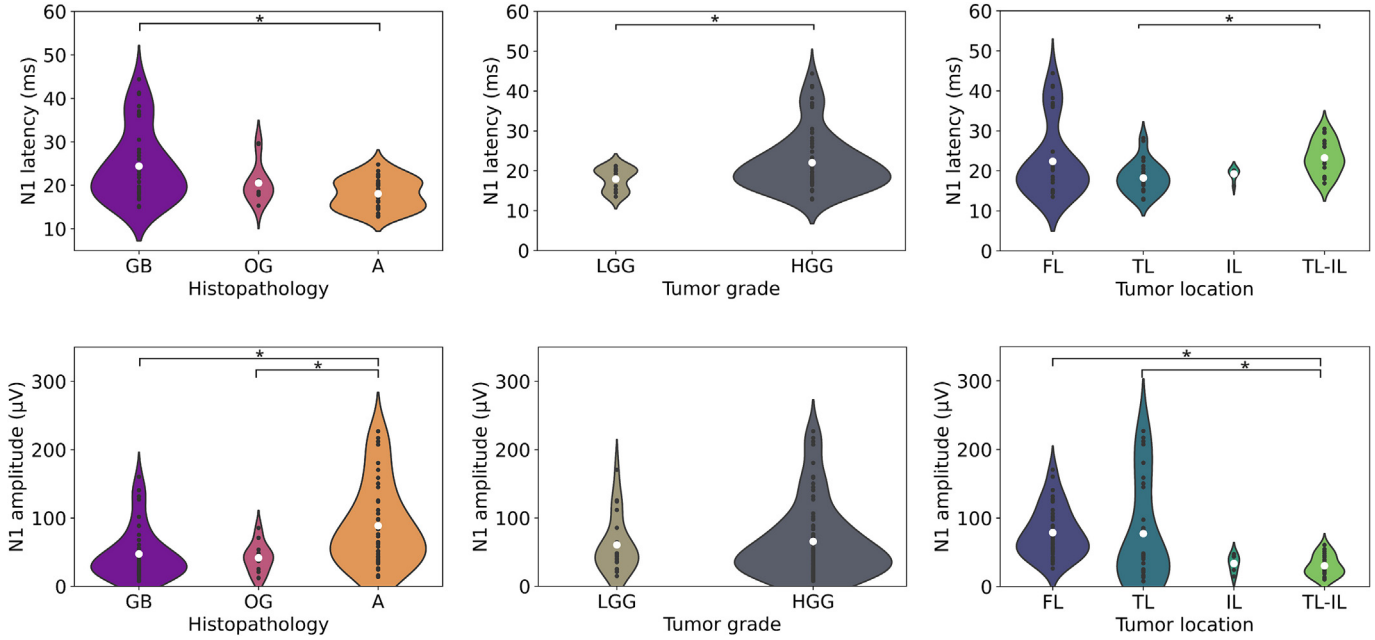

Fig. 4. N1 amplitude and latency differences in clinical features. Violin plot of the N1 amplitude and N1 latency distributions, showing the impact of histopathology (according to 2021 WHO classification), tumor grade and tumor location. *: statistical significance at $p < 0.05$. A: astrocytoma IDH mutated, FL: frontal lobe, GB: glioblastoma IDH wild type, HGG: high-grade glioma, IDH: Isocitratdehydrogenase, LGG: low-grade glioma, OG: oligodendroglioma IDH mutated, 1p/19q codeleted, TL: temporal lobe, IL: insular lobe, WHO: world health organization. © Inselspital, Bern University Hospital, Dept. of Neurosurgery.

p = 0.0003, Tukey post-hoc) (Fig. 4). There was also a significant difference in N1 amplitude depending on the histopathology (Kruskal-Wallis, p = 0.0003), with IDH wild type glioblastoma (47.3 ± 37.9 μV) giving rise to smaller amplitudes than IDH mutated astrocytoma (88.7 ± 59.9 μV). 1p/19q codeleted oligodendroglioma also had significantly lower N1 amplitudes (41.6 ± 21.4 μV) compared to IDH mutated astrocytoma but not compared to IDH wild type glioblastoma. Finally, IDH wild type glioblastoma had a significantly longer N2 latency (81.2 ± 19.8 ms) than 1p/19q codeleted oligodendroglioma (60.6 ± 4.4 ms) and IDH mutated astrocytoma (66.7 ± 15.4 ms) (ANOVA, p = 0.0007, Bonferroni post-hoc), whereas IDH wild type glioblastoma had significantly smaller N2 amplitudes (46.4 ± 34.1 μV) than astrocytoma (76.6 ± 51.5 μV) (Kruskal-Wallis, p = 0.006, Tukey post-hoc). Again, 1p/19q codeleted oligodendroglioma had significantly smaller N2 amplitudes (32.5 ± 11.1 μV) than IDH mutated astrocytoma, but no difference in comparison with IDH wild type glioblastoma. Note that there were fewer patients with 1p/19q codeleted oligodendroglioma than with IDH wild type glioblastoma or IDH mutated astrocytoma (see Table 1).

High-grade glioma significantly increased the N1 peak latency (22.0 ± 7.2 ms) compared to low-grade glioma (17.9 ± 2.8 ms) (Mann-Whitney, p = 0.016), but there was no significant difference in N1 amplitude between high-grade glioma (60.5 ± 40.6 μV) and low-grade glioma (65.6 ± 54.4 μV) (Fig. 4). High-grade glioma also significantly increased the N2 peak latency (75.8 ± 17.5 ms) compared to low-grade glioma (58.4 ± 12.3 ms) (Mann-Whitney, p = 0.001), but there was no significant difference in N2 amplitude between high-grade glioma (60.3 ± 44.9 μV) and low-grade glioma (57.3 ± 46.9 μV).

In the analysis of the effects of tumor location, temporo-insular tumors significantly increased N1 peak latency (23.2 ± 4.2 ms) compared to tumors in the temporal cortex (18.2 ± 3.9 ms), but there was no difference compared to frontal tumors (22.4 ± 8.9 ms) and insular tumors (19.2 ± 1.5 ms) (Kruskal-Wallis, p = 0.003, Tukey post-hoc) (Fig. 4). Furthermore, temporo-insular tumors led to smaller amplitudes (30.3 ± 15.1 μV) than frontal (78.6 ± 36.2 μV) and temporal tumors (77.2 ± 74.3 μV), but there was no difference compared to insular tumors (33.6 ± 12.2 μV) (Kruskal-Wallis, p = 5.76e-6, Tukey post-hoc). In addition, frontal tumors increased the N2 latency (78.2 ± 20.6 ms) compared to temporal (62.8 ± 8.0 ms) and insular tumors (51.6 ± 16.8 ms) (Kruskal-Wallis, p = 0.0003, Tukey post-hoc). However, tumor location had no significant influence on the N2 amplitude.

In the comparison between the sexes, females had significantly shorter N1 latencies (18.7 ± 5.2 ms) than males (22.2 ± 7.1 ms) (Mann-Whitney, p = 0.006). Females also had significantly higher N1 amplitudes (101.2 ± 63.7 μV) compared to males (48.0 ± 34.6 μV) (Mann-Whitney, p = 3.8e-5). Biological sex had no influence on N2 latency, but females had significantly higher N2 amplitudes (79.8 ± 48.8 μV) than males (47.1 ± 38.4 μV).

Furthermore, having a history of seizures seemed to decrease the N1 peak latency (19.6 ± 4.5 ms previous seizures, 23.7 ± 8.8 ms no previous seizures) (Mann-Whitney, p = 0.02); however, there was no significant difference in N1 amplitude, N2 latency and N2 amplitude between patients with a history of seizures and those without.

Patients who had postoperative aphasia had an increased N1 latency (24.8 ± 8.4 ms) in CCEPs recorded after resection compared to patients without postoperative aphasia (20.0 ± 6.0 ms) (Mann-Whitney, p = 0.027). Neither direct postoperative nor follow-up aphasia had an impact on N1 amplitude. N2 latency was increased in patients with postoperative aphasia in CCEPs recorded during (64.0 ± 12.6 ms) and after (86.7 ± 17.3 ms) resection compared to CCEPs recorded in patients without postoperative aphasia during (48.8 ± 14.2 ms) and after (65.7 ± 4.2 ms) resection, respectively (Student's t-test, p = 0.03 and p = 0.0004 respectively). Finally, CCEPs recorded after resection in patients with postoperative aphasia also showed a lower N2 amplitude (49.2 ± 31.9 μV) compared to patients without aphasia (94.0 ± 53.6 μV) (Student's t-test, p = 0.005).

Table 4
Review of studies on CCEPs during neurooncological surgeries.

Study	n	ndm	Pathology	Location	Awake CCEPs	Asleep CCEPs	BtW	WtB	Stimulation Parameters	Electrodes	Guide for optimal spots	Success rate	On/off analysis	N1 defintion	N1 peak latency (mean ± SD or range)	N1 amplitude (mean ± SD or range)	N2 definition
Yamao et al. 2014	6	6	LGG, HGG, O	IL, FL, TL, PL	6	6	6	0	Bp, A.C., PW: 0.3 ms. 1 Hz. 10–15 mA. 30 av.	Grid	fMRI, DTI FT	6 / 6	On/off	First negative peak at 20–40 ms	n/r	n/r	Late negative potential
Saito et al. 2014	13	13	LGG, HGG, O	IL, FL, PL	12	1	13	13	Bp, A.C., PW: 0.3 ms. 1 Hz. 3–8 mA. 100 av.	Strip	50 Hz stimulation	12 / 13	On/off	n/r (*)	83 ± 15 ms (*)	n/r	n/r
Tamura et al. 2016	5	5	LGG, HGG	FL, TL	5	0	0	5	Bp, A.C., PW: 0.3 ms. 1 Hz. Max. 15 mA. 30 av.	Grid	fMRI, DTI FT	5 / 5	On/off	n/r	55.4 ± 21.4 ms	58.02 ± 30.6 μV	n/r
Yamao et al. 2017	21	21	LGG, HGG, M, O	IL, FL, TL, PL	16	5	21	13	Bp, A.C., PW: 0.3 ms. 1 Hz. 10–15 mA. 30 av.	Grid	fMRI, DTI FT	21 / 21	On/off	n/r	27.9 ± 3.9 ms	n/r	n/r
Kanno et al. 2018	27	9	LGG, HGG, O	FL, TL, PL	0	17	17	17	Bp, A.C., PW: 0.3 ms. 1 Hz. 10 mA. 50 av.	Grid	Anatomy, Navigation	17 / 17	Off	Negative peak at 10–40 ms.	29 ± 3.2 ms	381.5 ± 29 μV	Late negative response
Suzuki et al. 2019	20	13	LGG, HGG	FL, TL, PL, TL-IL	13	13	13	13	Bp, A.C., PW: 0.3 ms. 1 Hz. 10 mA. 50 av.	Grid	Anatomy, Navigation	13 / 13	Off	First negative deflection distinguishable from stimulation artifact	25.1 (24.1–44.4) asleep, 22.5 (14.4–45.8) awake	133.9 (101.2–864) asleep, 168.8 (45.6–1485) awake	Late negative potential
Nakae et al. 2020	14	12	LGG, HGG, O	n/r	0	12	12	11	Bp, A.C., PW: 0.3 ms. 1 Hz. 15 mA. 30 av.	Grid	MRI, fMRI	12 / 12	On/off	Negative response larger than six times baseline SD	30.87–37.96 (**)	n/r	Late response
Yamao et al. 2021	14	13	LGG, HGG, O	IL, FL, TL, PL	13	13	13	0	Bp, A.C., PW: 0.3 ms. 1 Hz. 10–15 mA. 30 av.	Grid	Anatomy, Navigation	14 / 14	On/off	Negative response larger than six times baseline SD	28 ± 7.5 ms asleep, 27.3 ± 6.6 ms awake	323 ± 250.2 μV asleep, 338.5 ± 184.1 μV awake	n/r
Giampiccolo et al. 2021	9	9	HGG, O	FL, TL, PL	0	9	9	9	Bp, A.C., PW: 0.3–0.5 ms. 0.5–1 Hz. 20–30 mA.	Strip	DTI FT	5 / 9	Off	Negative peak at 15–40 ms.	21.3 ± 3.1 ms	43.4 ± 38 μV	n/r
Ishankulov et al. 2022	26	26	n/r	n/r	n/r	n/r	n/r	n/r	Biphasic. PW: 0.3 ms. 1 Hz. 3–4 mA, 30–50 av.	n/r	MRI, DTI FT	26 / 26	Off	n/r	n/r	n/r	n/r
Saito et al. 2022	7	7	LGG, HGG	IL, FL	7	0	7	0	Bp, biphasic, PW: 0.3 ms. 1 Hz. 6 mA. 100 av.	Strip	50 Hz stimulation	7 / 7	On	n/r	41.3 ± 22.2 (*, ***)	n/r	n/r
Vega-Zelaya et al. 2023	7	7	LGG, HGG, O	FL, FL-PL, TL-PL	1	7	7	7	Bp, current. PW: 1 ms. Max. 20 mA.	Grid	Anatomy, guided by train stimulation	7 / 7	On	Large upward peak	39 ± 0.7 ms WtB, 37.7 ± 0.8 μV BtW	204 ± 15.4 μV WtB; 184.1 ± 17 μV BtW	n/r
Kang et al. 2023	28	18	Glioma (n/r)	FL	0	18	18	0	n/r	n/r	Preoperative mapping	17 / 18	Off	n/r	n/r	n/r	n/r

(*): CCEP waveforms not called N1 or N2. CCEP is defined as the highest negative peak. (**): approximate values involving different parts of Broca's area and temporal language hubs. (***): mean and SD were calculated based on reported data.
A.C.: alternating current. Av: averages. Bp: bipolar. BtW: Broca to Wernicke. CCEPs: cortico-cortical evoked potentials. DTI: diffusion tensor imaging. FL: frontal lobe. (f)MRI: (functional) magnetic resonance imaging. FT: fiber tracking. HGG: high-grade glioma. IL: insular lobe. LGG: low-grade glioma. M: metastasis. n: number of included tumor surgeries. ndm: number of tumor surgeries in language-dominant hemisphere in which CCEPs were recorded. n/r: not reported. O: other pathologies. On/off: online/offline analysis. PL: parietal lobe. PW: pulse width. SD: standard deviation. TL: temporal lobe. WtB: Wernicke to Broca.

4. Discussion

Although initially introduced by Matsumoto et al. in epilepsy surgery (Matsumoto et al., 2004), CCEPs have recently been successfully recorded during tumor surgery. In addition to the 2 first reported series from Yamao et al. (2014) and Saito et al. (2014), we are aware of 13 studies that describe CCEPs recorded during tumor surgery. Table 4 summarizes some aspects of these studies. Although most of them included different tumor pathologies and tumor locations, the authors did not evaluate their effect on CCEP properties. Initially, CCEP monitoring was only performed during awake surgery or in a combined awake-asleep setting. Kanno et al. (2018), Nakae et al. (2020) and Giampiccolo et al. (2021a) were the first groups to successfully record CCEPs in patients operated on exclusively under general anesthesia. The first 2 groups used large grid arrays, while the third used strip electrodes, which they specifically guided by preoperative navigated transcranial magnetic stimulation (nTMS)-based fiber tracking. Saito et al. (2014, 2022) were the first group to guide their selective strip electrode placement with the help of intraoperative language mapping using Penfield stimulation, whereas Vega-Zelaya et al. (2023) guided their positioning using short-train motor mapping of the tongue area. Analyzing CCEPs, N1 is usually defined as the first negative deflection. The fact that this definition neither includes latency nor the possibility for inverted signals, leads to a large range of reported mean peak latencies (from 21 to 83 ms) of what the authors of the 13 studies we compared called N1 (see Table 4). Reported N1 amplitudes were either not available or varied considerably between studies. The definition of N2 was less frequently reported. This heterogeneity among studies hampers the identification of normative data on CCEP properties when trying to introduce CCEPs into a clinical routine.

Taking into account these observations on previous studies, we highlight some aspects of our series, which might facilitate integration of CCEPs in a neurooncological surgical context. In our series, CCEPs were recorded in 95% of attempts, which illustrates the feasibility of the technique. Our series contained 36% patients with low-grade glioma and 64% with high-grade glioma, demonstrating that the technique can also be used in patients with peritumoral edema and an infiltrative tumor growth pattern. This is important because patients who have high-grade glioma with peritumoral edema are usually less suitable for an awake craniotomy (Nossek et al., 2013; Spena et al., 2017). To our knowledge, ours is the first attempt to compare CCEP properties in patients with different tumor entities. Interestingly, in our cohort of patients with IDH wild type glioblastoma, N1 and N2 latency were increased and N1 and N2 amplitude decreased when compared to patients with IDH mutated astrocytoma, although the effect was lost when compared to 1p/19q codeleted oligodendroglioma (Fig. 4). However, the comparatively low number of patients with 1p/19q codeleted oligodendroglioma in our series may have biased these results. Grouping all high-grade and all low-grade gliomas revealed a significant lengthening of N1 and N2 latencies in high-grade tumors. This might be due to peritumoral edema and thus, prolonged N1 and N2 latencies could be a marker for altered connectivity. Furthermore, tumor patients with a history of preoperative seizures had a significantly shorter N1 latency, which might hint at hyperexcitability in patients with epilepsy. However, these are only a preliminary results, which require further investigation.

We observed that tumor location affected CCEP features. Tumors involving insula areas tended to increase N1 latency and significantly decrease N1 amplitudes compared to other tumor locations (Fig. 4). Even if the neurophysiological source of N1 remains unclear, this could be an additional indication for involvement of the peri-insular tracts, which may be conducting these potentials. Interestingly, Yamao et al. stimulated the white matter of the presumed AF and recorded CCEPs at the cortical surface of both ends of the pathway (Yamao et al., 2014). The summation of the 2 latencies was equal to the latency of surface stimulation with cortical recordings. Similar observations have recently been reported by Rossel et al., who used axono-cortical evoked potentials to establish markers for white matter connectivity (Rossel et al., 2023).

Patients who exhibited postoperative aphasia showed a significantly delayed N1 and N2 latency of CCEPs recorded after tumor resection. This indicates that CCEPs might serve as a surrogate marker for altered connectivity of the AF or other language tracts. However, unlike previously reported studies (Saito et al., 2014; Saito et al., 2022; Vega-Zelaya et al., 2023; Yamao et al., 2017), we did not observe a significantly lower N1 amplitude but rather a significantly lower N2 amplitude in patients with postoperative aphasia. Those previous series had compared N1 amplitude alterations in the same patient whereas we compared differences of amplitudes across different patients. Since post-resection CCEPs are altered in patients with postoperative aphasia, this is further evidence that CCEPs are possible surrogate markers for the integrity of language pathways. However, further studies with larger patient cohorts are needed for a definitive interpretation, especially regarding the correlation of different aphasia types with alterations of CCEP features. Indeed, this is important since more than one tract contributes to language. It has been suggested that the AF is associated with phonological encoding (Duffau et al., 2003b; Giampiccolo and Duffau, 2022; Usui et al., 2003), the inferior fronto-occipital fascicle (IFOF) with semantic control (Duffau et al., 2005), and the superior longitudinal fascicle (SLF) III with anarthria (Fridriksson et al., 2013; Gajardo-Vidal et al., 2021).

Curiously, we observed a shorter N1 latency and higher N1 amplitude in CCEPs in female than in male patients. To our knowledge, no previous study has investigated this aspect in CCEPs. However, sex differences in the AF and associative language pathways have been the focus of some imaging studies (Catani et al., 2007; Forkel et al., 2014; Lebel and Beaulieu, 2009), and, if confirmed, such a difference could explain our observations.

Unlike many previously reported series, which used grid arrays on a broadly exposed cortex (Kanno et al., 2018; Nakae et al., 2020; Suzuki et al., 2019; Tamura et al., 2016; Vega-Zelaya et al., 2023; Yamao et al., 2014, 2017, 2021), we performed minimally invasive approaches, with craniotomies centered over the tumor and, if the targeted eloquent cortex was not exposed, we pushed 4-contact strip electrodes under the dura (Fig. 1). Therefore, the technique is feasible without altering the surgical approach and concept. One of our goals was to implement CCEP recordings without interfering with the surgical routine, and we are confident that this achievement can set an example for other neurosurgical centers wishing to adopt this technique.

Many previous studies (Kanno et al., 2018; Nakae et al., 2020; Suzuki et al., 2019; Tamura et al., 2016; Yamao et al., 2014, 2017, 2021) reported the placement of large grids for stimulation and recording based on functional magnetic resonance imaging (fMRI) data, neuronavigation, or anatomy (Table 4). Most start with the patient asleep, stimulating frontal areas and recording from temporal sites. The temporal spot with the highest amplitude is then used for reciprocal stimulation to obtain bidirectional recordings. During a later step of the surgery, they validate their CCEP responses by Penfield stimulation. However, the selection of optimal spots is not guided by Penfield stimulation in these cases. So it is possible that they do not distinguish the specific tracts that are involved in generating these potentials (Giampiccolo et al., 2021b). To overcome this obstacle, Giampiccolo et al. (2021a) guided their electrode placement using preoperative language

mapping performed with nTMS and fiber tracking from the hot spots, which were integrated into the neuronavigation system. However, in no step of the surgery was the awake patient tested with Penfield stimulation, which might have contributed to their lower success rate in obtaining CCEP responses (5 out of 9 patients, 56%). In contrast, we guided our selective stimulation and selective recordings by anatomical landmarks, DTI fiber tracking and importantly, by intraoperative Penfield speech mapping. We chose our optimal spots according to our intraoperative functional results. In this manner, we tried to make certain that the signals obtained originated solely from language tracts. In other words, we attempted to make sure that the CCEPs were generated from a physiological structure involved in speech/language performance (Giampiccolo et al., 2023). A further indication of the neurophysiological nature of our responses comes from the fact that no CCEPs were recorded in neighboring contacts of the optimal sites (for an example see Fig. 2). Thus, we were able to exclude current spread or recording of far-field potentials.

As explained above, we attempted to record selectively from language tracts. In this regard, the latencies, amplitudes, and other characteristics of the CCEPs we collected may help guide the gathering of CCEP data in tumor patients (Table 2). In the entire cohort, there was no significant difference in P1, N1, P2, and N2 latency between the awake and asleep settings while stimulating from Broca and recording from Wernicke (Table 3). However, when restricting to CCEPs elicited at Wernicke and recorded from Broca, there was a difference in latency between the awake and asleep settings. This could have been due to the smaller number of CCEPs recorded in the WtB group. Previously published articles (Suzuki et al., 2019; Yamao et al., 2021) describe a decrement in N1 amplitude of around 25–30% during the change from awake to asleep settings. We observed the same tendency but it did not reach statistical significance (Table 3). However, in most cases, we compared cohorts (interpatient) and not individual patients (intrapatient) during the awake and asleep phases.

Whereas previous studies mostly defined "N1" as the first negative deflection (see Table 4 for an overview of the different definitions of N1), we chose to define N1 as a negative deflection occurring at a peak latency between 10 and 30 ms and with a duration of at least 10 ms. The signal was inverted for analysis if there was a notable positive deflection at these latencies. This is because we included bipolar recordings of CCEPs, so the electrode montage can affect the polarity of the signal. We even observed a few inverted N1 recordings in referential montages. This could be because a CCEP mirror image is recorded if the negative CCEP is generated from the sulcal part. This would be similar to the N20/P20 phase reversal recordings of median nerve somatosensory evoked potentials (SSEP) ((Rossel et al., 2023) and Matsumoto, personal communication). An example can be seen in the bipolar recordings between W1-W2 and W2-W3 in the illustrated case of Fig. 2. In any case, defining the N1 simply as the first negative peak (without inverting the trace) might explain why Saito et al. (2014) and Tamura et al. (2016) described either very late N1 peaks or only one negative peak in their recordings. In our whole series, bipolar recordings were more successful than referential recordings (90% versus 75%). Thus, bipolar recordings might be more efficient for obtaining CCEPs, and we encourage neurophysiologists to include them in their protocol.

In our series of patients, we were more successful in recording CCEPs from BtW than WtB (90% versus 54%). Matsumoto et al. (2004) provide a possible explanation by suggesting that the AF is more convergent in Broca's area and more divergent (spread out) in Wernicke's area. Thus, when stimulating in Wernicke's area, the responses in Broca's area are expected to be smaller in amplitude and more localized. By contrast, stimulating in Broca's area leads to more dispersed responses in Wernicke's area, which have higher amplitude. This might be why it is easier to select the initial stimulation site in the frontal region, which is also in line with our higher success rate of BtW versus WtB. However, Vega-Zelaya et al. observed significantly higher CCEP amplitudes in WtB than BtW (Vega-Zelaya et al., 2023). We are unaware of any other studies that explicitly evaluated the difference in their CCEP amplitudes depending on the direction of stimulation. Our cohort did not exhibit any significant difference in N1 amplitude or latency comparing BtW and WtB. If reproducible, it would be noteworthy if bidirectional, i.e. orthodromic and antidromic CCEP responses can be recorded without significant latency differences. Currently, an additional point of scientific debate is the low conduction velocity of the AF (Lemaréchal et al., 2022), as well as the potential involvement of synaptic connections in the generation of N1. However, this is beyond the scope of the present article.

Another noteworthy feature of our clinical protocol is the real-time availability of unprocessed data to the surgical team via a screen. There was thus immediate feedback for the surgeon when the strip electrode needed to be repositioned. Unlike many other groups (Giampiccolo et al., 2021a; Ishankulov et al., 2022; Kang et al., 2023; Kanno et al., 2018; Suzuki et al., 2019), we were able to use online recordings without post-processing. This might be a first step toward the future implementation of continuous CCEP monitoring during tumor resection. However, the correlation of intraoperative signal changes to clinical outcomes needs to be investigated and demonstrated on a larger scale before this can become a reality. In addition, more fundamental research needs to be done to understand the different CCEP components (mainly N1 and N2) and their neurophysiological generators (synaptic versus axonal versus combined) to provide reliable feedback to the surgical team (Keller et al., 2014).

5. Limitations

We did not use CCEPs for continuous functional monitoring during surgery, even though previous studies show that 3 clinical centers have already tried this (Nakae et al., 2020; Saito et al., 2014, 2022; Vega-Zelaya et al., 2023; Yamao et al., 2014, 2021). In the few reported surgeries where this was done, the classical neurophysiological cut-off of a 50% amplitude decrement was used to predict a permanent language deficit. However, clear warning criteria, such as the percentage of amplitude decrease or latency prolongation, still need to be validated. Establishing normative data for different cohorts, including for asleep and awake surgeries and for various tumor pathologies or tumor locations, is essential to achieve this goal.

Unfortunately, we changed the filter setting in the last 2 cases. This is why these patients' data were excluded from the statistical analysis. The hardware and software filters substantially impact the shape and properties of the recorded signals (Luck, 2014). Since the main frequency of our signals ranged from 10 to about 30 Hz, it stands to reason that lowering the high-pass filter (which was set at 30 Hz in all the cases analyzed) will lead to higher amplitudes at these frequencies in the future. This effect was observed in the last 2 patients included in this study when we changed to a high-pass filter of 0.5 Hz. The resulting difference in amplitudes and latencies led us to exclude them from the data analysis. This also means that the absolute value of N1 and N2 characteristics reported in the present paper (Table 2) can only be expected with comparable filter settings. Due to its long waveform duration, the N2 contributes to lower frequencies and its amplitude is therefore especially affected by a higher high-pass filter. Given that a filter typically suppresses amplitude logarithmically, a low cut-off frequency of 30 Hz means that between 30 Hz and one order of magnitude lower (3 Hz) the amplitude of the signal is not yet suppressed

dramatically. However, everything lower than 3 Hz is reduced by several orders of magnitude. The precise steepness of the decline in gain depends on the filter type and parameters (Luck, 2014), which are unfortunately unavailable in the device specifications. Further, artifacts due to inadequate filter settings can mimic CCEPs, as illustrated by Vega-Zelaya et al. (see (Vega-Zelaya et al., 2023), Fig. 1). Given these observations, it is important to highlight the importance of training and experience in neurophysiology to differentiate artifacts from true neurophysiological responses. This is essential to obtain high quality CCEP recordings. For instance, an observed phase reversal might be an additional indication that the recorded CCEP is a real neurophysiological response and not just stimulation artifact (Fig. 2).

With a total of 20 patients, our study population was small. However, we controlled for several clinical aspects, as highlighted in Table 1. We focused on patients with high- and low-grade glioma with tumors in the dominant hemisphere and no severe aphasia. Further, we tried to focus on one single fiber tract connection between frontal and temporal speech areas (likely the AF) and our selective recordings were functionally guided by intraoperative speech testing. As mentioned in the methods, each patient contributed from 1 to 12 CCEPs depending on available and repeatable recordings in various settings (awake vs asleep, BtW vs WtB, referential vs bipolar recordings, and 2 trials for repeatability). Thus, the data pool is unbalanced, but after the selection process, we used a total of 97 CCEPs for clinical correlations.

6. Conclusion

Based on our series of 20 glioma patients, we report a correlation of clinical aspects with CCEP characteristics. Optimal stimulation and recording sites were guided by awake Penfield stimulation and analyzed in real time during surgery. We observed no significant difference in amplitude and latency when comparing CCEPs recorded awake versus asleep or depending on the direction of stimulation and recording (BtW versus WtB). However, CCEPs were affected by tumor involvement of the insula and high-grade histopathology, especially IDH wild type glioblastoma. Properties of CCEPs recorded after tumor resection correlated with short- and long-term postoperative aphasia. Thus, CCEPs could be used as surrogate markers for altered connectivity of language tracts. Further, we obtained our data during minimally invasive approaches with craniotomies centered over the tumor, without changing the surgical approach, and providing direct feedback to the surgeon. Hence, this study demonstrates the feasibility of real-time CCEP recordings without any need to alter the craniotomy size. As such, our study may help guide the incorporation of CCEP recording in intraoperative neurophysiological monitoring.

Funding

None.

Conflict of interest

None of the authors has potential conflicts of interest to be disclosed related to this study.

Acknowledgements

We would like to thank Anja Giger for supplying the illustrations and Susan Kaplan for language editing. We would like to dedicate this manuscript to the memory of Vedran Deletis, who sadly passed away during the review process. He was one of the leading figures in intraoperative neurophysiology, ever curious, willing to push the boundaries, open to new ideas and new technologies that could help improve the safety of patients in the operating room. He will continue to inspire the field.

Appendix A. Supplementary data

Supplementary data to this article can be found online at https://doi.org/10.1016/j.clinph.2023.12.136.

References

Ashburner J, Friston KJ. Unified segmentation. Neuroimage 2005;26(3):839–51.
Berger MS, Ojemann GA. Intraoperative brain mapping techniques in neuro-oncology. Stereotact Funct Neurosurg 1992;58(1–4):153–61.
Binder JR. The Wernicke area: Modern evidence and a reinterpretation. Neurology 2015;85(24):2170–5.
Catani M, Allin MP, Husain M, Pugliese L, Mesulam MM, Murray RM, et al. Symmetries in human brain language pathways correlate with verbal recall. PNAS 2007;104(43):17163–8.
Duffau H, Capelle L, Denvil D, Sichez N, Gatignol P, Taillandier L, et al. Usefulness of intraoperative electrical subcortical mapping during surgery for low-grade gliomas located within eloquent brain regions: functional results in a consecutive series of 103 patients. J Neurosurg 2003a;98(4):764–78.
Duffau H, Gatignol P, Denvil D, Lopes M, Capelle L. The articulatory loop: study of the subcortical connectivity by electrostimulation. Neuroreport 2003b;14(15):2005–8.
Duffau H, Gatignol P, Mandonnet E, Peruzzi P, Tzourio-Mazoyer N, Capelle L. New insights into the anatomo-functional connectivity of the semantic system: a study using cortico-subcortical electrostimulations. Brain 2005;128(4):797–810.
Forkel SJ, Thiebaut de Schotten M, Dell'Acqua F, Kalra L, Murphy DG, Williams SC, et al. Anatomical predictors of aphasia recovery: a tractography study of bilateral perisylvian language networks. Brain 2014;137(7):2027–39.
Fridriksson J, Guo D, Fillmore P, Holland A, Rorden C. Damage to the anterior arcuate fasciculus predicts non-fluent speech production in aphasia. Brain 2013;136(11):3451–60.
Gajardo-Vidal A, Lorca-Puls DL, Team P, Warner H, Pshdary B, Crinion JT, et al. Damage to Broca's area does not contribute to long-term speech production outcome after stroke. Brain 2021;144(3):817–32.
Giampiccolo D, Cattaneo L, Sala F. Untangling wave characteristics in direct axono-cortical evoked potentials to understand cortico-cortical evoked potentials. Clin Neurophysiol 2023;S1388–2457(23):00647–8.
Giampiccolo D, Duffau H. Controversy over the temporal cortical terminations of the left arcuate fasciculus: a reappraisal. Brain 2022;145(4):1242–56.
Giampiccolo D, Parmigiani S, Basaldella F, Russo S, Pigorini A, Rosanova M, et al. Recording cortico-cortical evoked potentials of the human arcuate fasciculus under general anaesthesia. Clin Neurophysiol 2021a;132(8):1966–73.
Giampiccolo D, Parmigiani S, Basaldella F, Russo S, Pigorini A, Rosanova M, et al. Reply to 'Intraoperative cortico-cortical evoked potentials for monitoring the arcuate fasciculus: feasible under general anesthesia?'. Clin Neurophysiol 2021b;133:177–8.
Hamer PDW, Robles SG, Zwinderman AH, Duffau H, Berger MS. Impact of intraoperative stimulation brain mapping on glioma surgery outcome: a meta-analysis. J Clin Oncol 2012;30(20):2559–65.
Ishankulov T, Danilov G, Pitskhelauri D, Titov OY, Ogurtsova A, Buklina S, et al. Prediction of postoperative speech dysfunctions in neurosurgery based on cortico-cortical evoked potentials and machine learning technology. Sovrem Tekhnologii Med 2022;14(1):25–32.
Kang KM, Kim KM, Kim IS, Kim JH, Kang H, Ji SY, et al. Functional magnetic resonance imaging and diffusion tensor imaging for language mapping in brain tumor surgery: validation with direct cortical stimulation and cortico-cortical evoked potential. KJR 2023;24(6):553.
Kanno A, Enatsu R, Ookawa S, Noshiro S, Ohtaki S, Suzuki K, et al. Interhemispheric asymmetry of network connecting between frontal and temporoparietal cortices: a corticocortical-evoked potential study. World Neurosurg 2018;120:e628–36.
Keller SS, Crow T, Foundas A, Amunts K, Roberts N. Broca's area: nomenclature, anatomy, typology and asymmetry. Brain Lang 2009;109(1):29–48.
Krieg SM, Lioumis P, Mäkelä JP, Wilenius J, Karhu J, Hannula H, et al. Protocol for motor and language mapping by navigated TMS in patients and healthy volunteers; workshop report. Acta Neurochir 2017;159:1187–95.
Kuklisova-Murgasova M, Aljabar P, Srinivasan L, Counsell SJ, Doria V, Serag A, et al. A dynamic 4D probabilistic atlas of the developing brain. NeuroImage 2011;54(4):2750–63.
Lebel C, Beaulieu C. Lateralization of the arcuate fasciculus from childhood to adulthood and its relation to cognitive abilities in children. Hum Brain Mapp 2009;30(11):3563–73.
Lemaréchal J-D, Jedynak M, Trebaul L, Boyer A, Tadel F, Bhattacharjee M, et al. A brain atlas of axonal and synaptic delays based on modelling of cortico-cortical evoked potentials. Brain 2022;145(5):1653–67.
Louis DN, Perry A, Wesseling P, Brat DJ, Cree IA, Figarella-Branger D, et al. The 2021 WHO classification of tumors of the central nervous system: a summary. Neuro Oncol 2021;23(8):1231–51.

Luck SJ. An introduction to the event-related potential technique. MIT press; 2014.
Matsumoto R, Kunieda T, Nair D. Single pulse electrical stimulation to probe functional and pathological connectivity in epilepsy. Seizure 2017;44:27–36.
Matsumoto R, Nair DR, LaPresto E, Najm I, Bingaman W, Shibasaki H, et al. Functional connectivity in the human language system: a cortico-cortical evoked potential study. Brain 2004;127(10):2316–30.
Nakae T, Matsumoto R, Kunieda T, Arakawa Y, Kobayashi K, Shimotake A, et al. Connectivity gradient in the human left inferior frontal gyrus: intraoperative cortico-cortical evoked potential study. Cereb Cortex 2020;30(8):4633–50.
Nossek E, Matot I, Shahar T, Barzilai O, Rapoport Y, Gonen T, et al. Failed awake craniotomy: a retrospective analysis in 424 patients undergoing craniotomy for brain tumor. J Neurosurg 2013;118(2):243–9.
Rossel O, Schlosser-Perrin F, Duffau H, Matsumoto R, Mandonnet E, Bonnetblanc F. Short-range axono-cortical evoked-potentials in brain tumor surgery: waveform characteristics as markers of direct connectivity. Clin Neurophysiol 2023.
Saito T, Muragaki Y, Tamura M, Maruyama T, Nitta M, Tsuzuki S, et al. Monitoring cortico-cortical evoked potentials using only two 6-strand strip electrodes for gliomas extending to the dominant side of frontal operculum during one-step tumor removal surgery. World Neurosurg 2022;165:e732–42.
Saito T, Tamura M, Muragaki Y, Maruyama T, Kubota Y, Fukuchi S, et al. Intraoperative cortico-cortical evoked potentials for the evaluation of language function during brain tumor resection: initial experience with 13 cases. J Neurosurg 2014;121(4):827–38.
Spena G, Schucht P, Seidel K, Rutten G-J, Freyschlag CF, D'Agata F, et al. Brain tumors in eloquent areas: a European multicenter survey of intraoperative mapping techniques, intraoperative seizures occurrence, and antiepileptic drug prophylaxis. Neurosurg Rev 2017;40:287–98.
Stieglitz LH, Seidel K, Wiest R, Beck J, Raabe A. Localization of primary language areas by arcuate fascicle fiber tracking. Neurosurg 2012;70(1):56–65.
Suzuki Y, Enatsu R, Kanno A, Yokoyama R, Suzuki H, Tachibana S, et al. The influence of anesthesia on corticocortical evoked potential monitoring network between frontal and temporoparietal cortices. World Neurosurg 2019;123:e685–92.
Szelényi A, Bello L, Duffau H, Fava E, Feigl GC, Galanda M, et al. Intraoperative electrical stimulation in awake craniotomy: methodological aspects of current practice. Neurosurg Focus 2010;28(2):E7.
Tadel F, Baillet S, Mosher JC, Pantazis D, Leahy RM. Brainstorm: a user-friendly application for MEG/EEG analysis. Comput Intell Neurosci 2011;2011:1–13.
Tamura Y, Ogawa H, Kapeller C, Prueckl R, Takeuchi F, Anei R, et al. Passive language mapping combining real-time oscillation analysis with cortico-cortical evoked potentials for awake craniotomy. J Neurosurg 2016;125(6):1580–8.
Usui K, Ikeda A, Takayama M, Matsuhashi M, Yamamoto JI, Satoh T, et al. Conversion of semantic information into phonological representation: a function in left posterior basal temporal area. Brain 2003;126(3):632–41.
Vega-Zelaya L, Pulido P, Sola RG, Pastor J. Intraoperative Cortico-Cortical Evoked Potentials for Monitoring Language Function during Brain Tumor Resection in Anesthetized Patients. JIN 2023;22(1):17.
Vincent M, Guiraud D, Duffau H, Mandonnet E, Bonnetblanc F. Electrophysiological brain mapping: Basics of recording evoked potentials induced by electrical stimulation and its physiological spreading in the human brain. Clin Neurophysiol 2017;128(10):1886–90.
Yamao Y, Matsumoto R, Kunieda T, Arakawa Y, Kobayashi K, Usami K, et al. Intraoperative dorsal language network mapping by using single-pulse electrical stimulation. Hum Brain Mapp 2014;35(9):4345–61.
Yamao Y, Matsumoto R, Kunieda T, Nakae T, Nishida S, Inano R, et al. Effects of propofol on cortico-cortical evoked potentials in the dorsal language white matter pathway. Clin Neurophysiol 2021;132(8):1919–26.
Yamao Y, Suzuki K, Kunieda T, Matsumoto R, Arakawa Y, Nakae T, et al. Clinical impact of intraoperative CCEP monitoring in evaluating the dorsal language white matter pathway. Hum Brain Mapp 2017;38(4):1977–91.
Keller CJ, Honey CJ, Mégevand P, Entz L, Ulbert I, Mehta AD. Mapping human brain networks with cortico-cortical evoked potentials. Philos Trans R Soc Lond B Biol Sci 2014;369(1653), 20130528. https://doi.org/10.1098/rstb.2013.0528.